



DLR Contribution to the first High Lift Prediction Workshop – Part I

R. Rudnik, S. Melber-Wilkending, S. Crippa

**DLR, Institute of Aerodynamics and Flow Technology,
38108, Braunschweig, Germany**

D-

- **Extend validation and verification of the DLR TAU-code's predictive capabilities for a 'new' 3D high lift test case**
- **Benchmark hybrid unstructured grid generation approaches, namely CENTAUR/TAU vs. SOLAR/TAU for a 3D high lift configuration**
 - **consideration of gridding guidelines for high lift cases**
 - **check prism-dominant vs. hex-dominant near wall grid topologies**
 - **grid refinement study for 3D configuration**
- **Check/improve best practice approaches for complex high lift configurations**
 - **turbulence model performance**
 - **convergence start-up procedure**
 - **efficiency aspects, simplifications (e.g. b.t.e. resolution)**

⇒ **Focus on CENTAUR-TAU and case 1**

CASE 1

CENTAUR/TAU

CENTAUR Grid Family

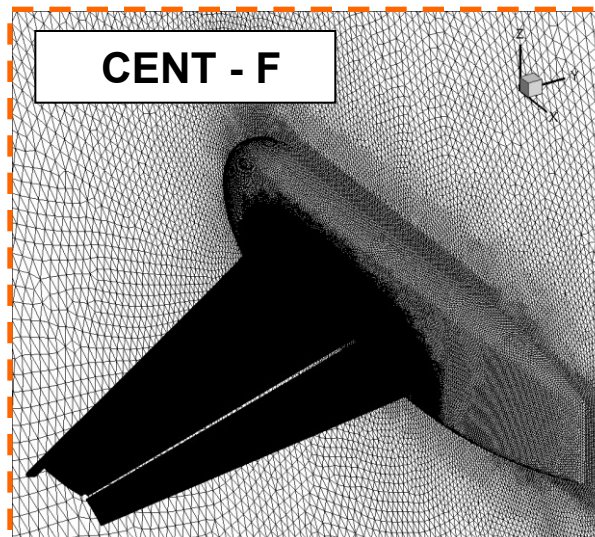
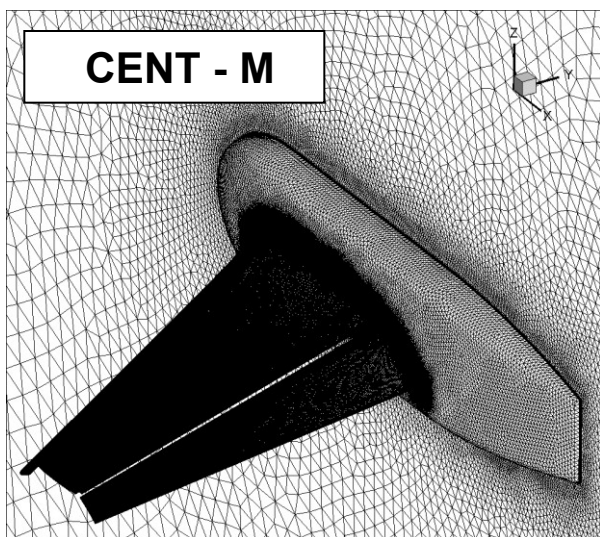
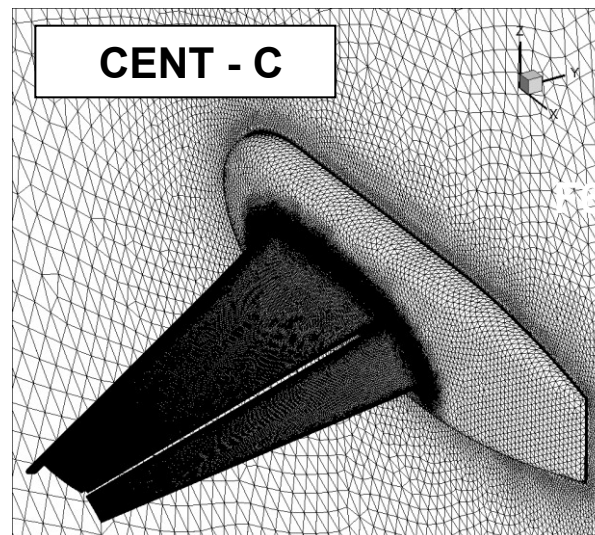
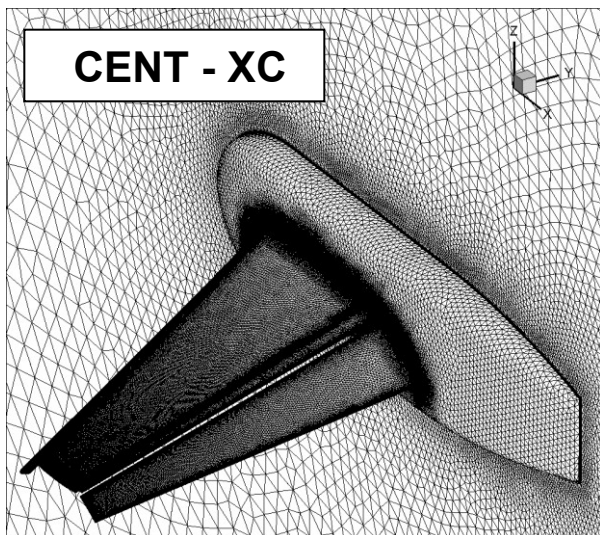
- Grid family approach with 3 levels (initially 4)
- Grid level characteristics

Grid Level	Pts.	Prisms	Surf. Elem.	Tot. Elem.
XC	12,923,391	19,288,488	695,194	37,418,633
C	16,374,761	26,509,026	865,844	43,548,725
M	31,498,984	53,614,403	1,596,988	78,725,517

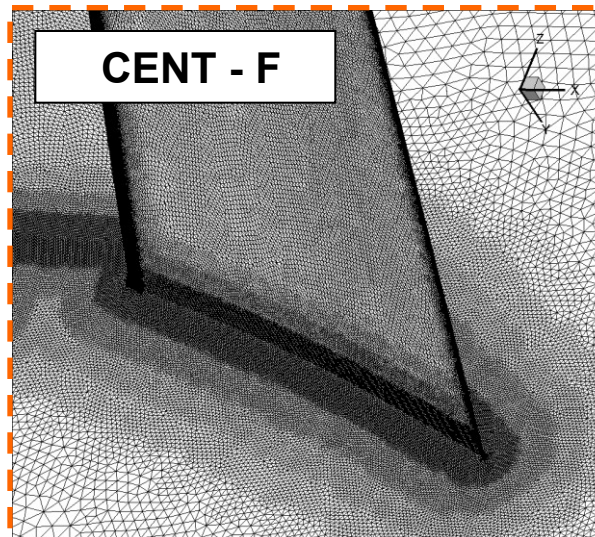
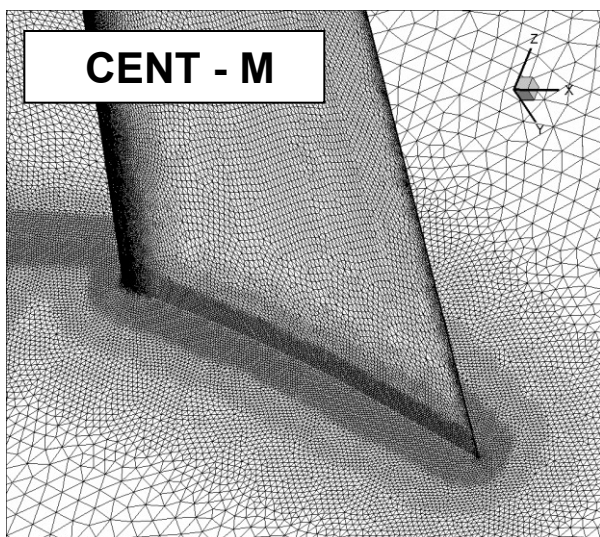
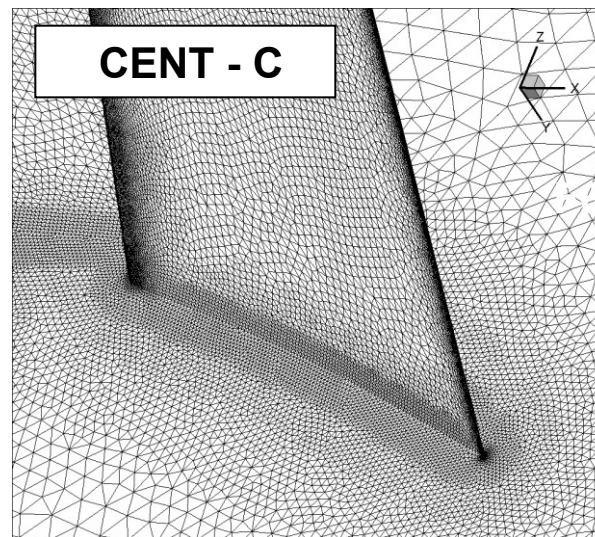
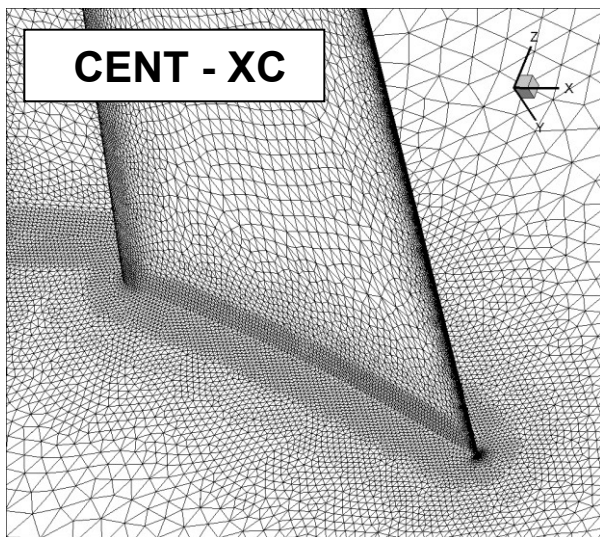
- Grid generation and adaptation approach
 - y^+ -adaptation sectionwise and spanwise
 - adjustment of prism layer thickness sectionwise and spanwise
 - spanwise adaptation of streamwise surface resolution at l.e. and t.e.
 - additional refinement by local cylinder sources along trim curves at root and tip

- **Grid generation approach – HiLiftPW-special features / lessons learned**
 - **B.t.e. resolution requires CAD-repatching on t.e. to account for specif. resolution (cut, reorganize and join in 50 spanwise section)**
 - **Parametric Source Control in order to better**
 - **introduce sectionwise requirements along span**
 - **control wall normal stretching of prisms and surface resolution requirements**
 - **to achieve smooth cell growth distribution**
 - **automated transfer to different grid levels**
 - **allow for handling of multiple (~2.000+) single grid sources**
- **DLR fine grid problem using CENTAUR:**
 - **surface and near wall areas successfully resolved with prisms**
 - **outer prism layer characterized by large cell (surface) aspect ratios**
 - **failure to connect with tets due to cell AR and requirement for constant volume ratio**
 - **automatic ability to locally adjust number of prisms, spanwise anisotropy and surface resolution**

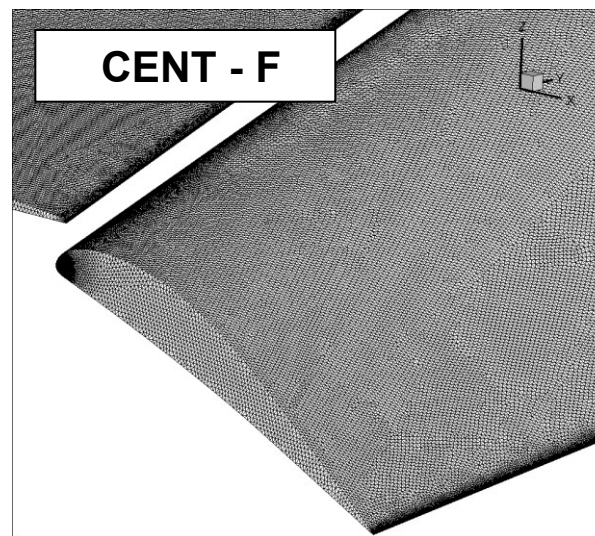
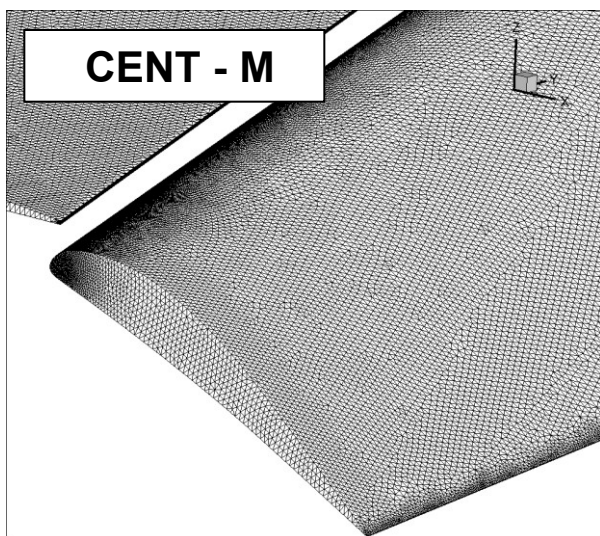
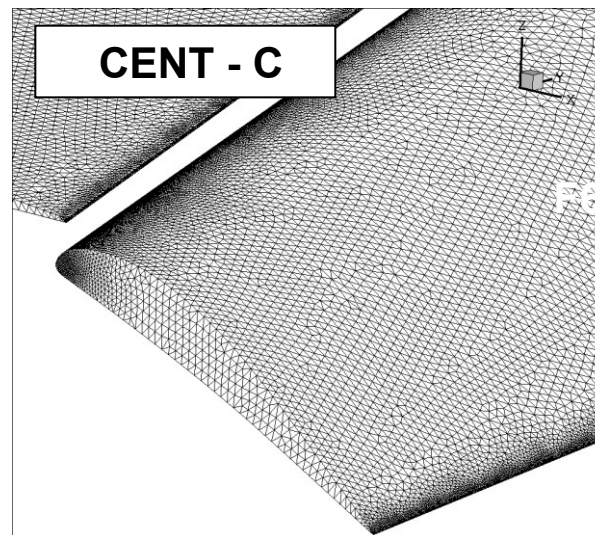
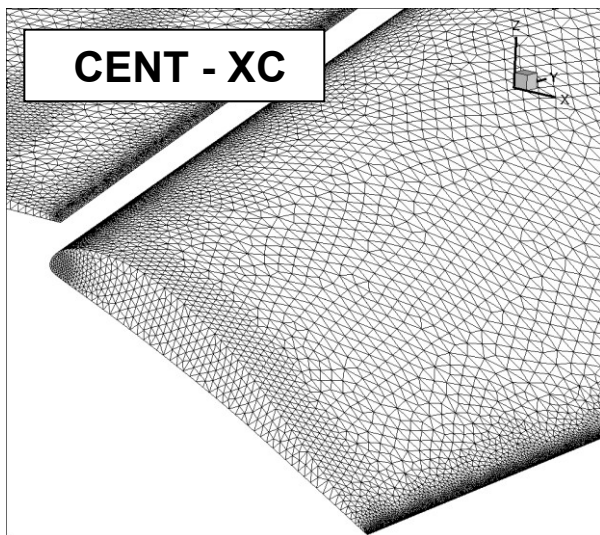
- Surface grid - configuration - rear view



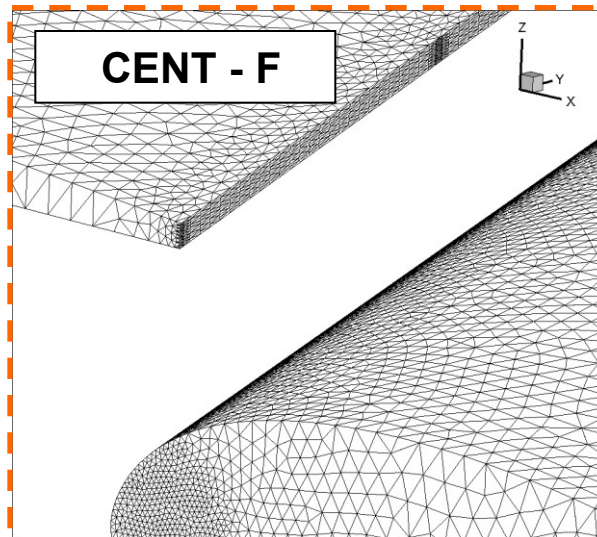
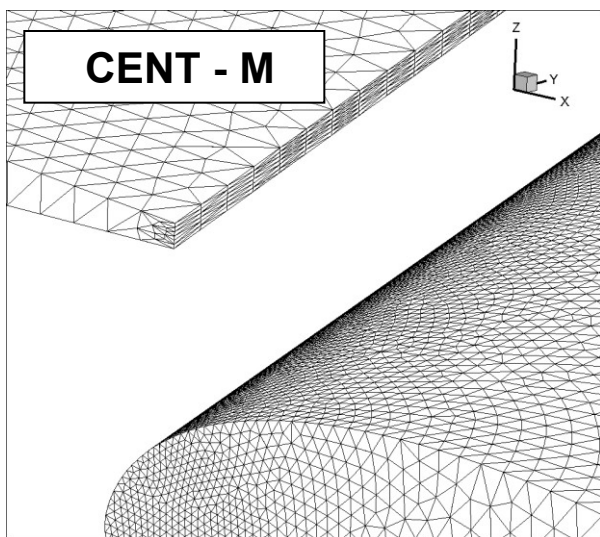
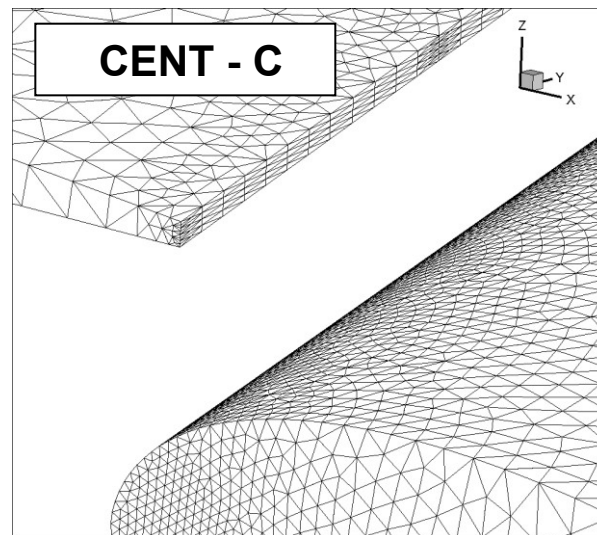
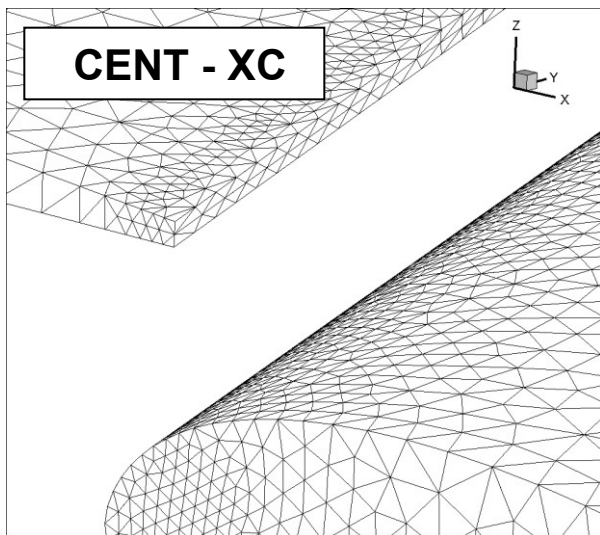
- Surface grid - WB-junction flap - lower side view



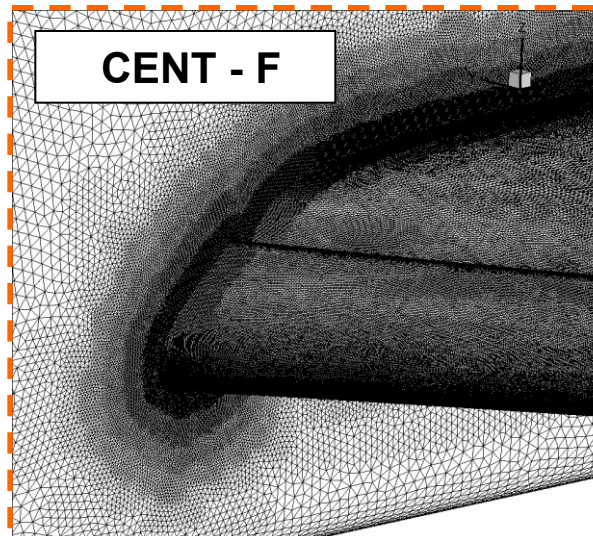
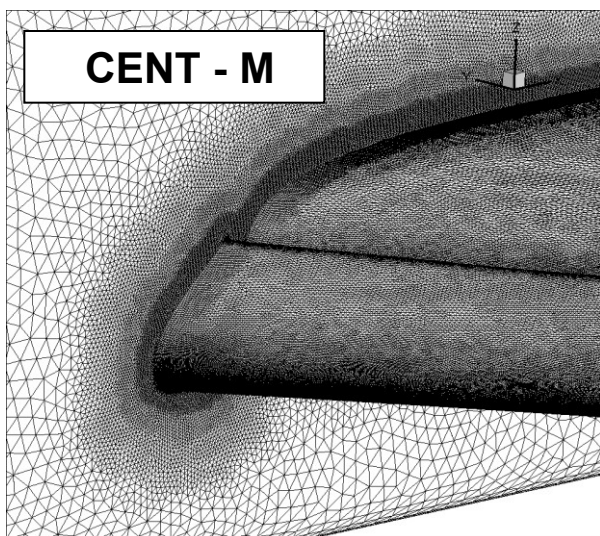
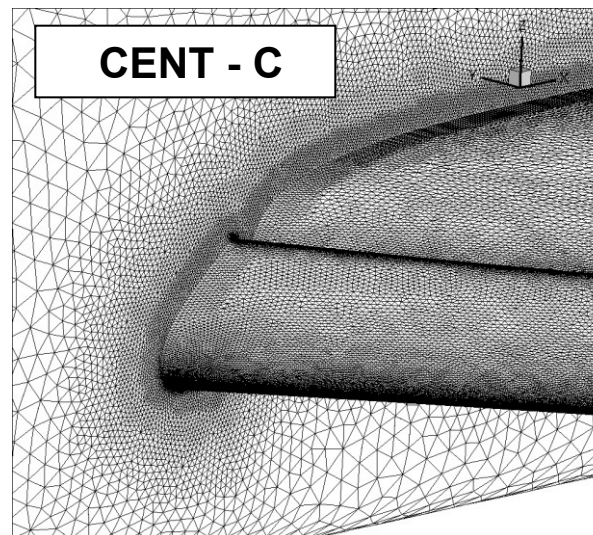
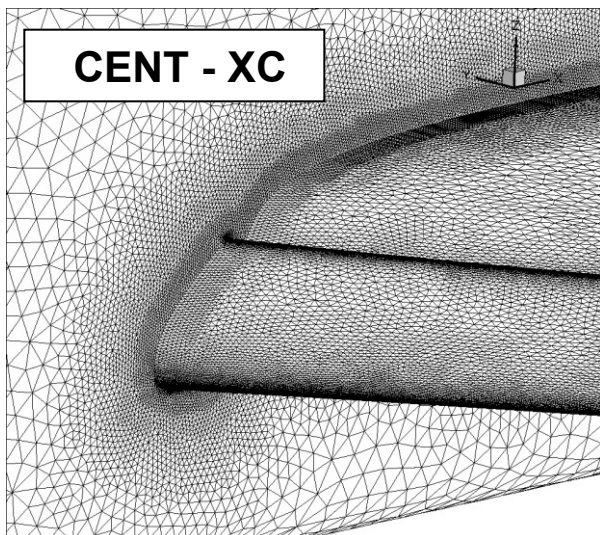
- Surface grid - flap tip - upper side view



- Surface grid – wing t.e., flap gap - upper side view



- Surface grid - WB-junction, slat, wing - upper side view



CASE 1

CENTAUR/TAU

Baseline CFD Results – Medium grid

- **Code Version:** DLR TAU code 2010.1.0

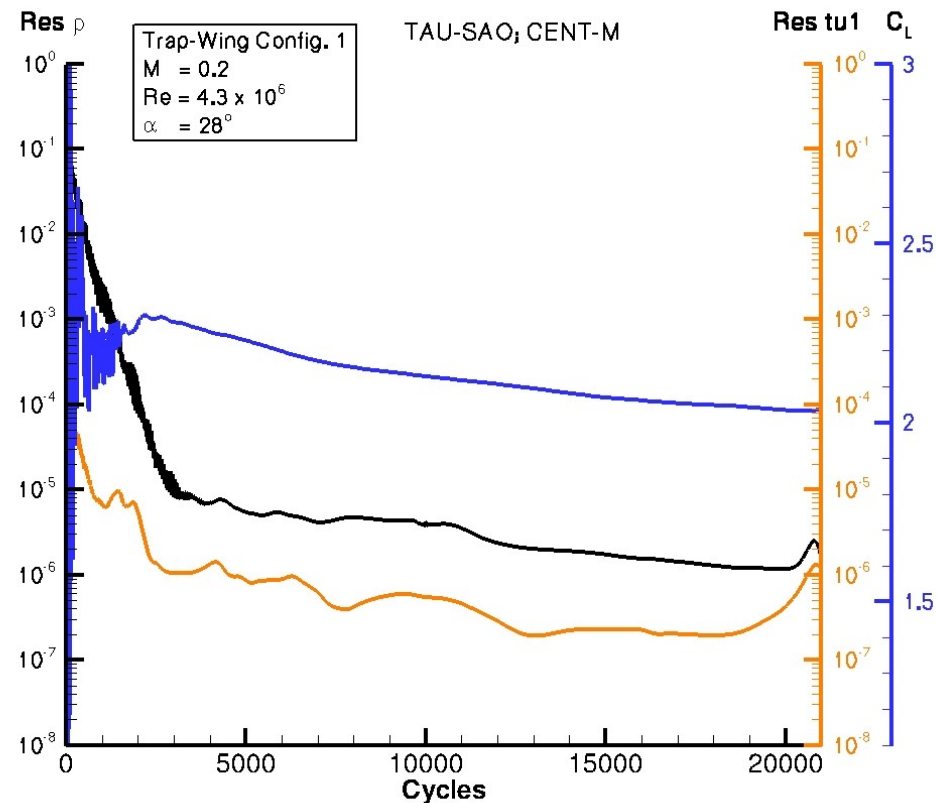
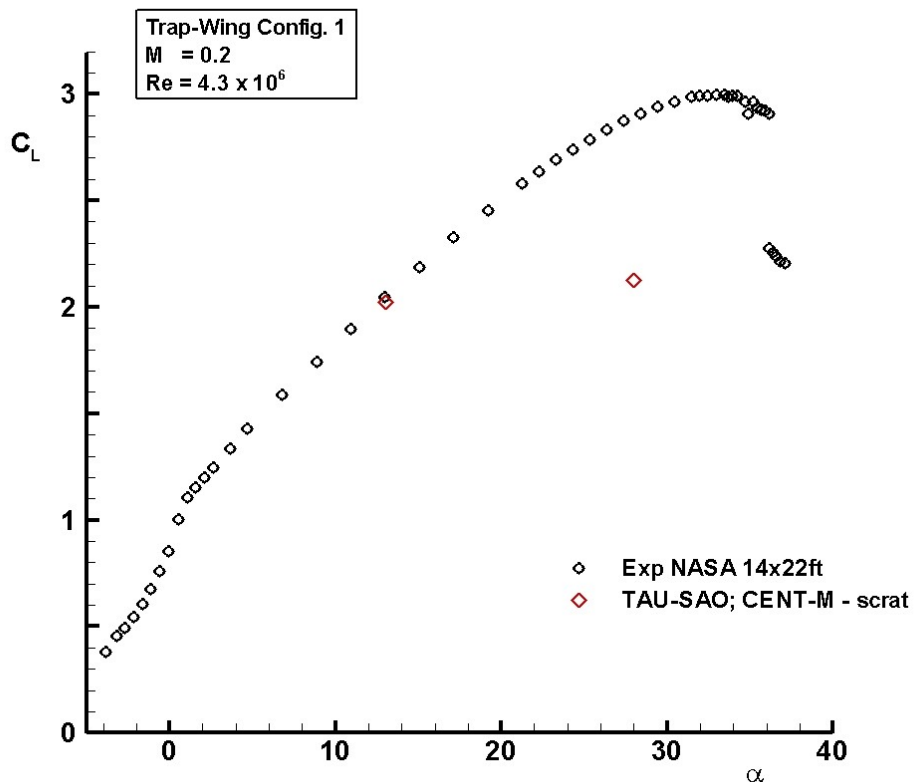
- **Spatial Discretization:**
 - **Main equations:** Jameson central, 2nd order;
Blend scalar (80%) – matrix (20%) dissipation

 - **Turb. Equations:** Roe upwind, 2nd order

- **Turbulence Models:**
 - Spalart-Allmaras, original formul. (SAO)
 - Menter k- ω SST (SST)
 - SSG/LRR- ω diff. Re-stress model (RSM)

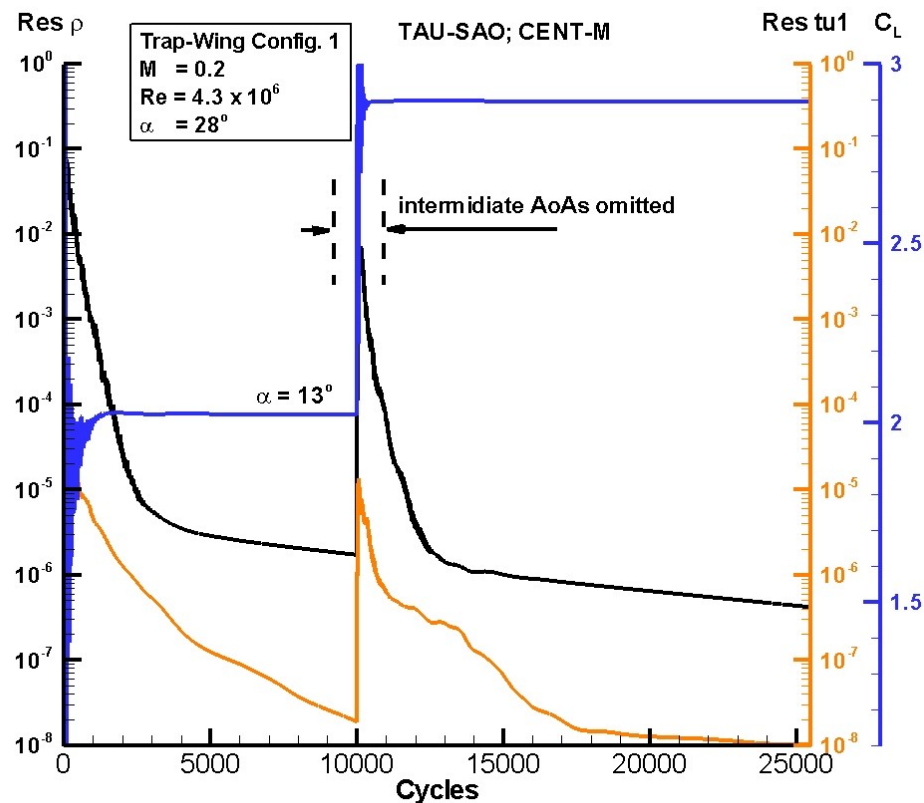
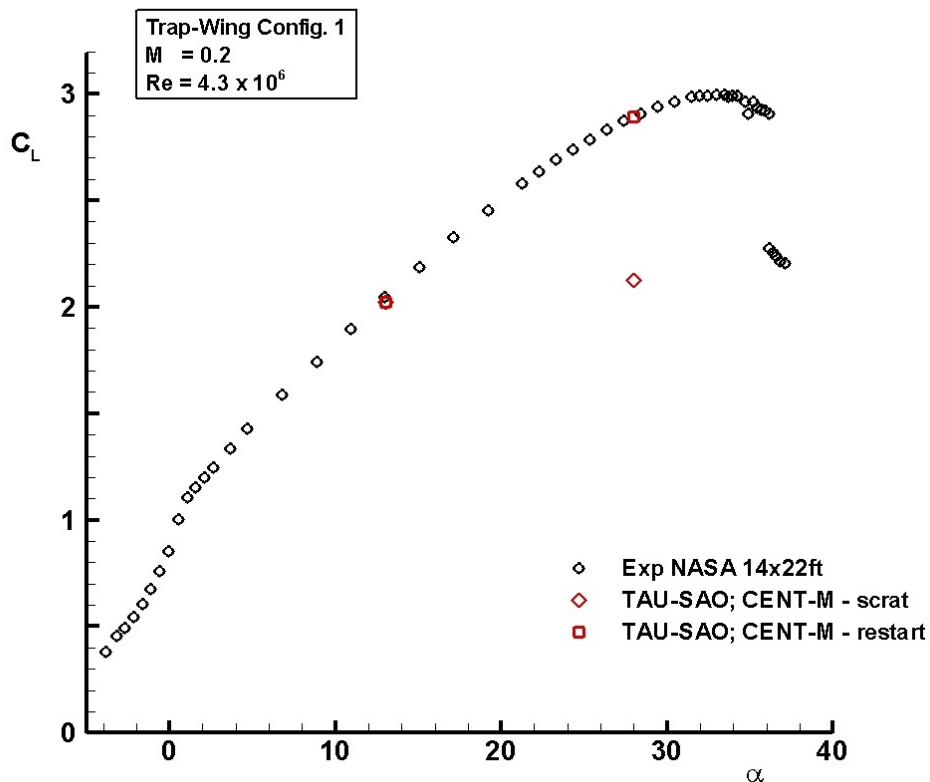
- **Temp. Integration:**
 - LU-SGS Backward Euler
 - Multigrid, 3V cycle

- TAU-SAO, grid-m; $\alpha = 13, 28^\circ$ start-up procedure: scratch

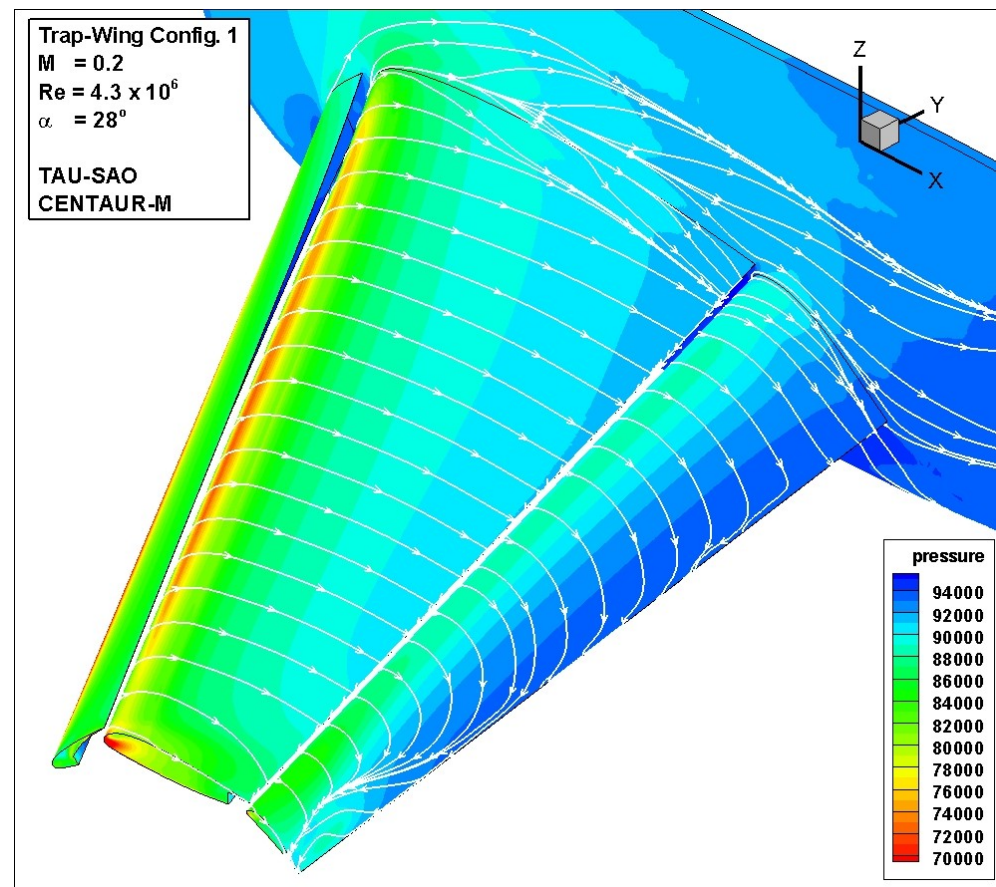
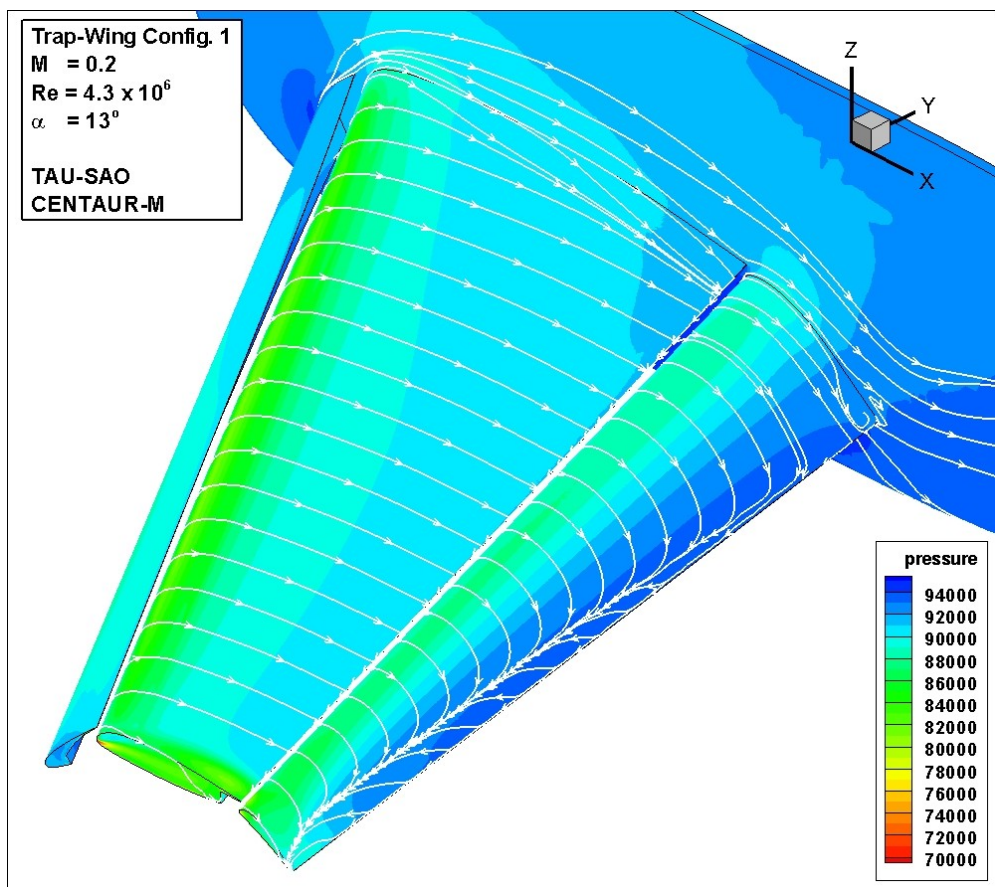


- TAU-SAO, grid-m; $\alpha = 13, 28^\circ$

start-up procedure stepwise restart ($\Delta\alpha = 2^\circ$)

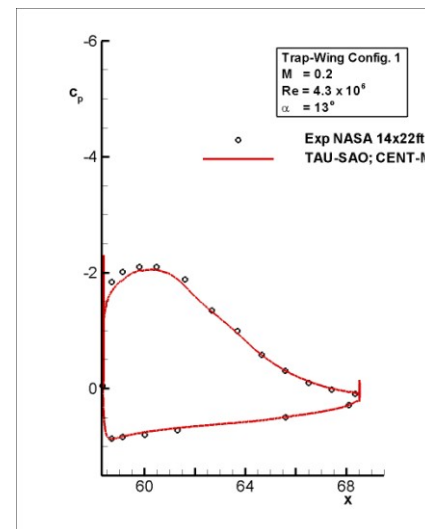
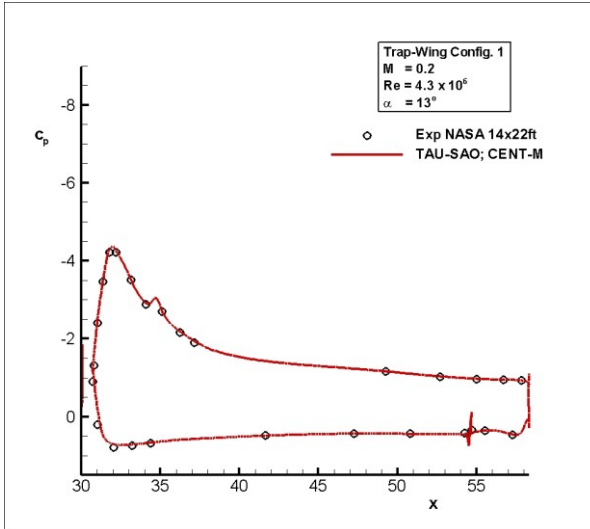
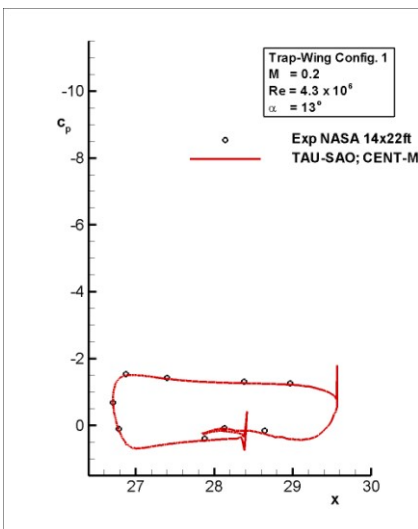


- TAU-SAO, grid-m; $\alpha = 13, 28^\circ$: isobars and surface streamlines

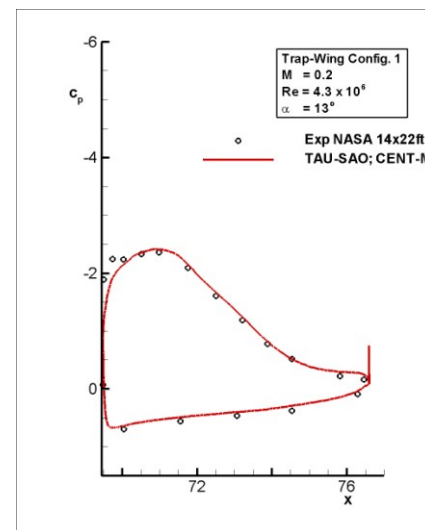
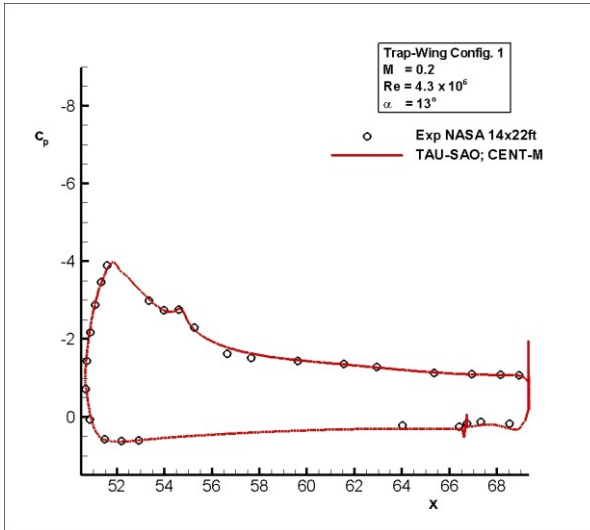
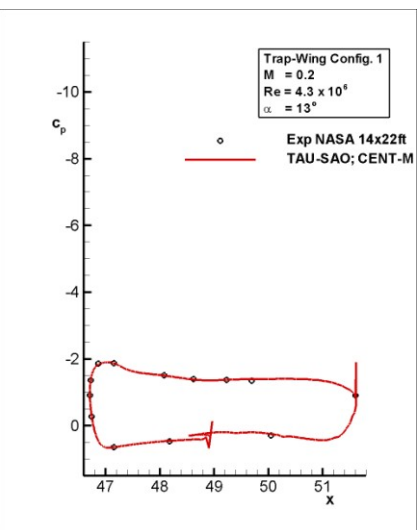


- TAU-SAO, grid-m; $\alpha = 13^\circ$:

pressure distribution at



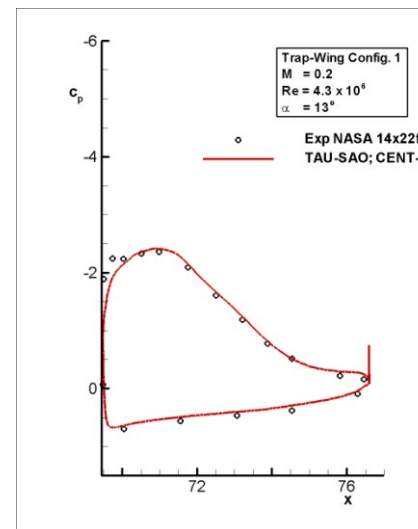
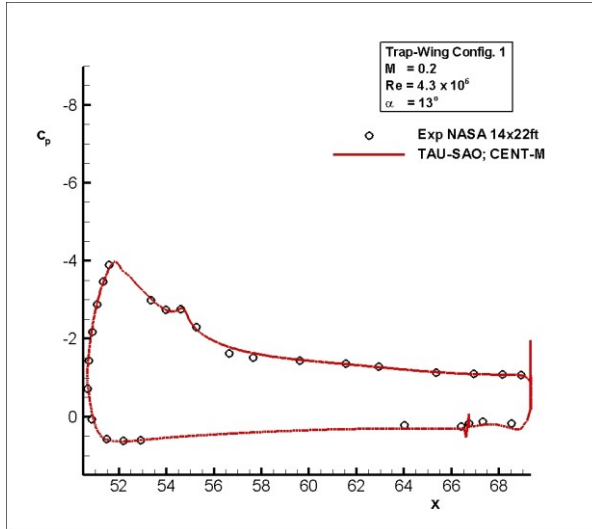
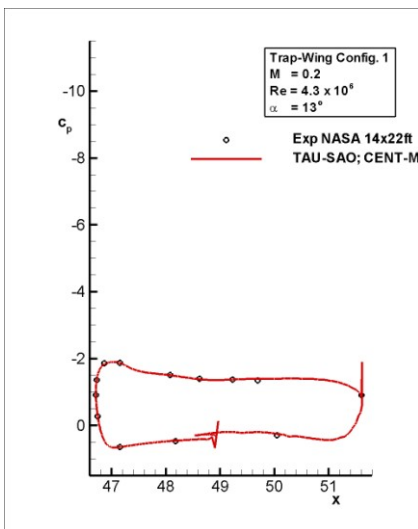
$\eta = 0.50$



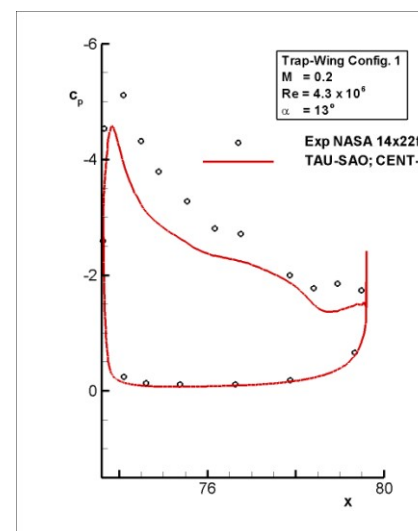
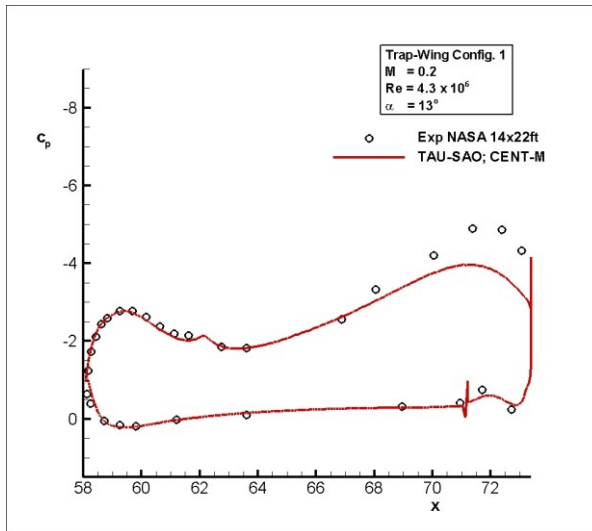
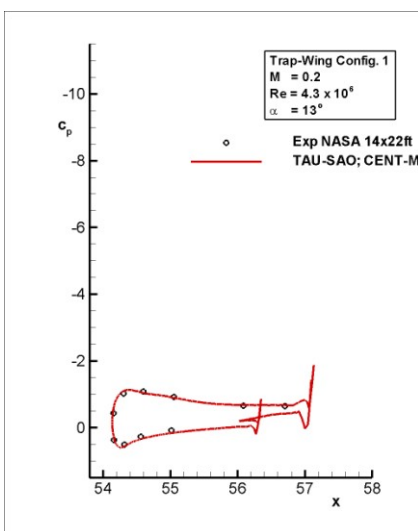
and 0.85

- TAU-SAO, grid-m; $\alpha = 13^\circ$:

pressure distribution at



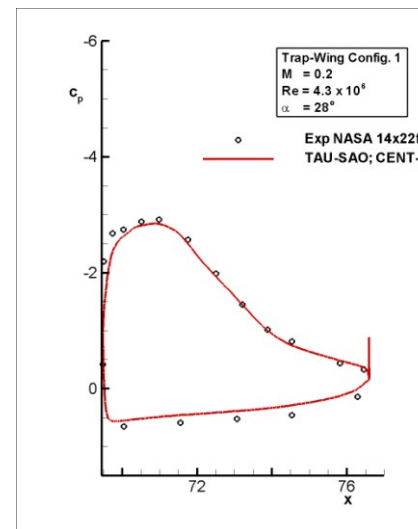
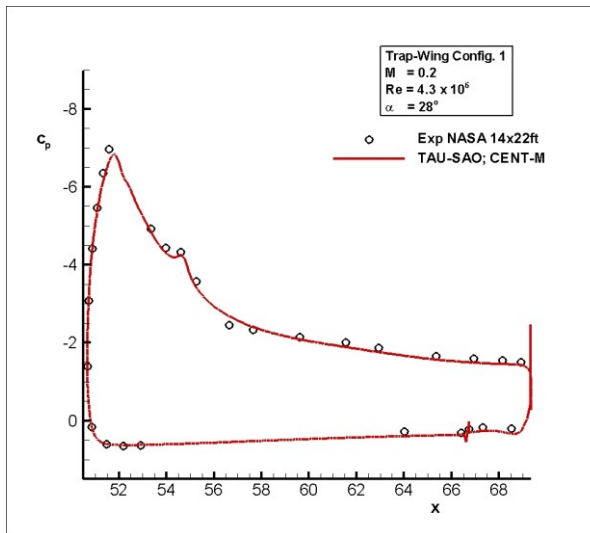
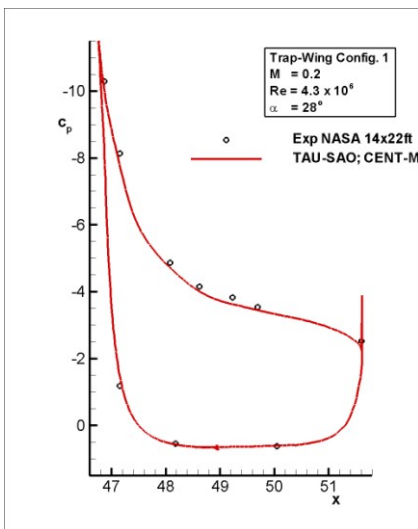
$\eta = 0.85$



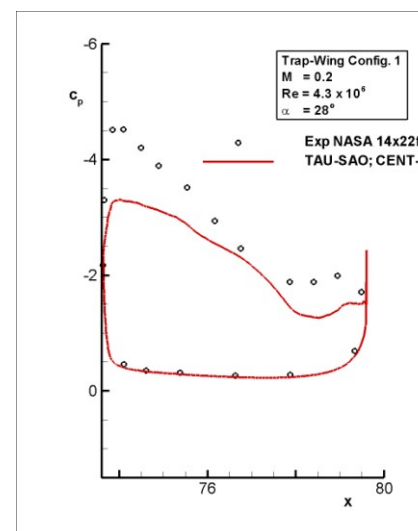
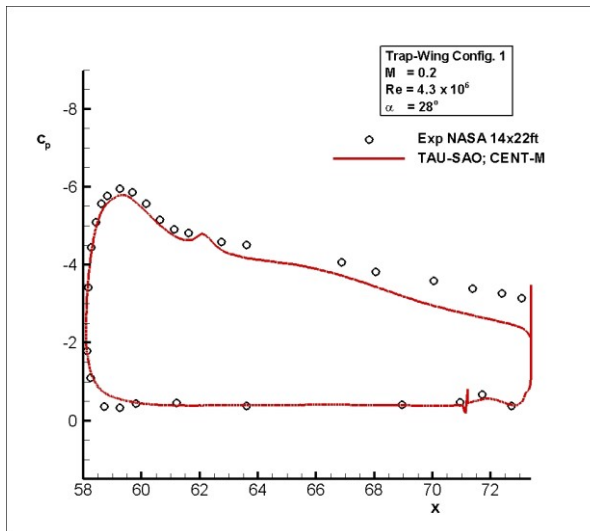
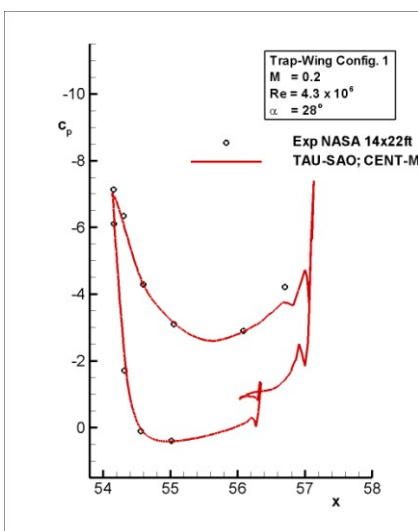
and 0.98

- TAU-SAO, grid-m; $\alpha = 28^\circ$:

pressure distribution at

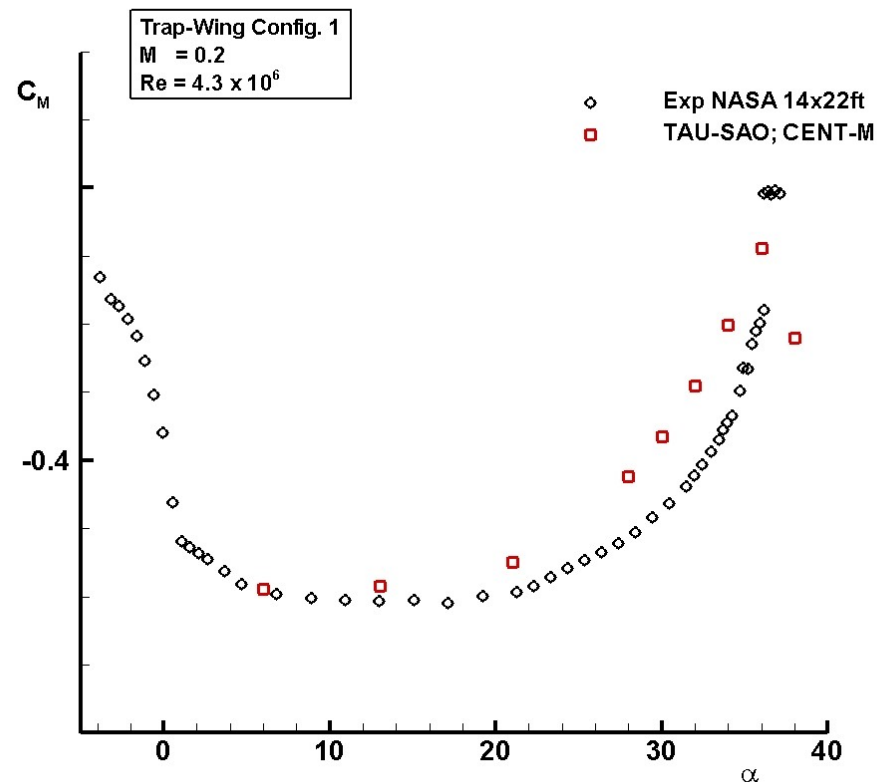
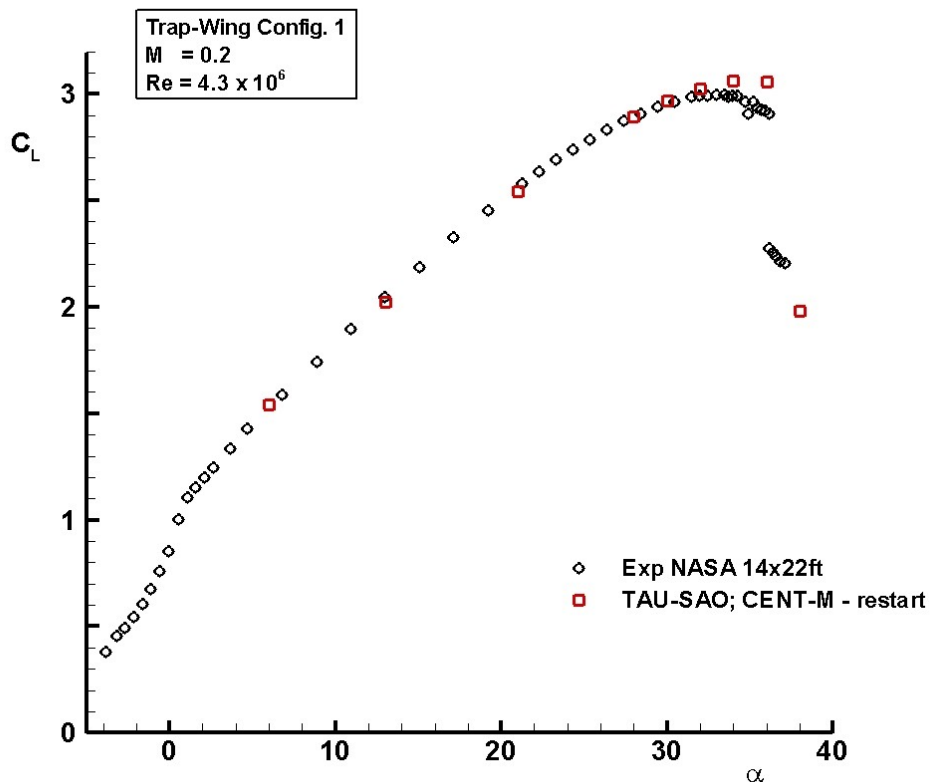


$\eta = 0.85$



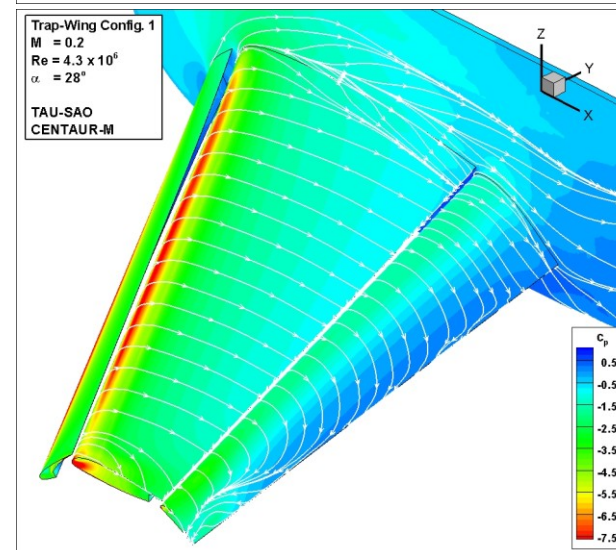
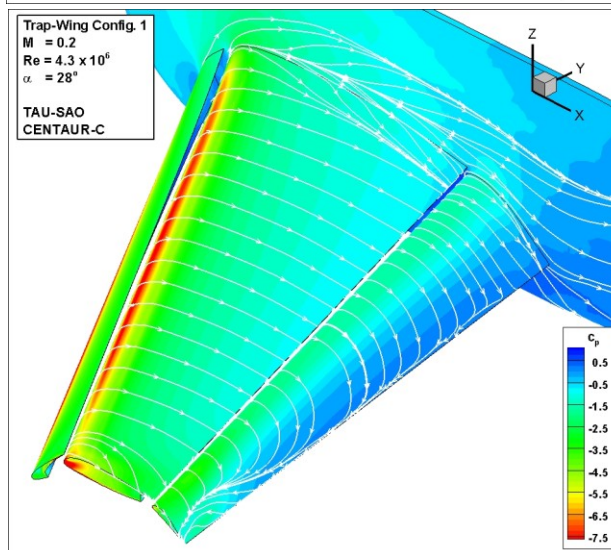
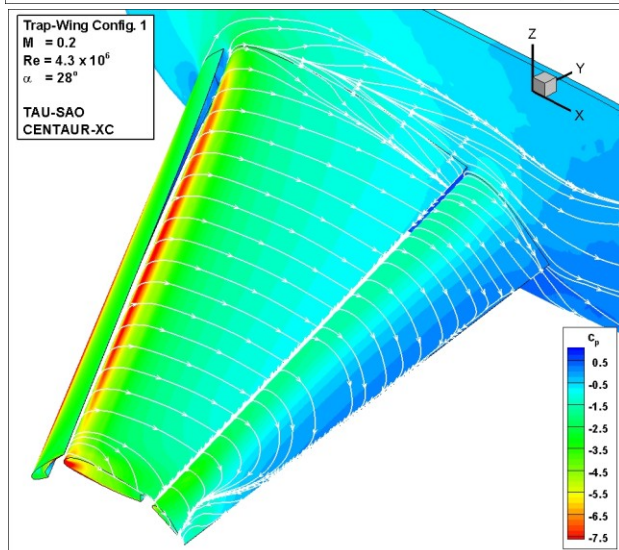
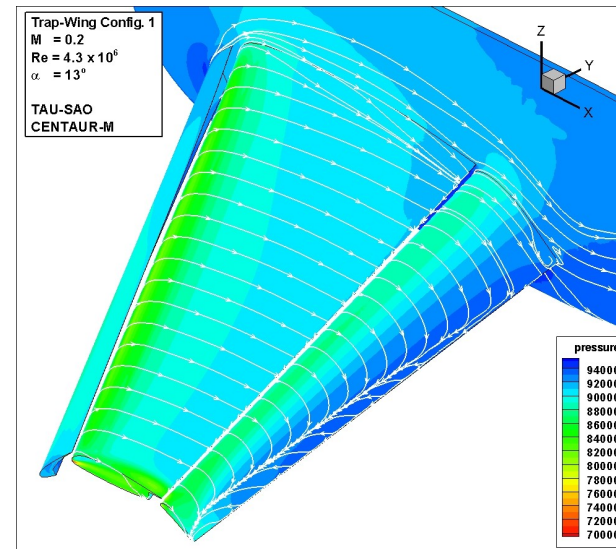
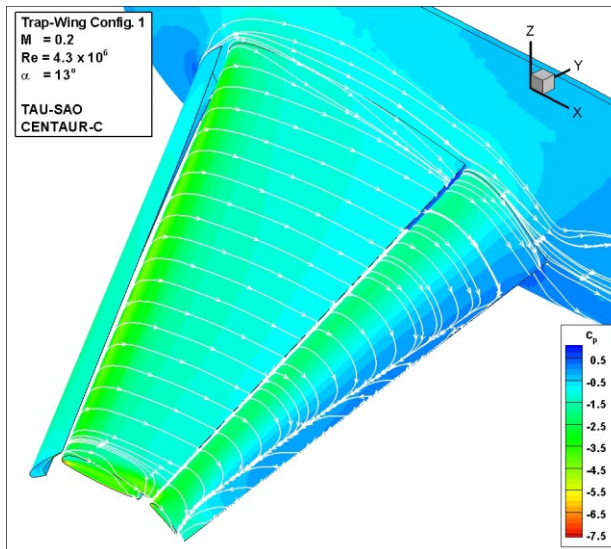
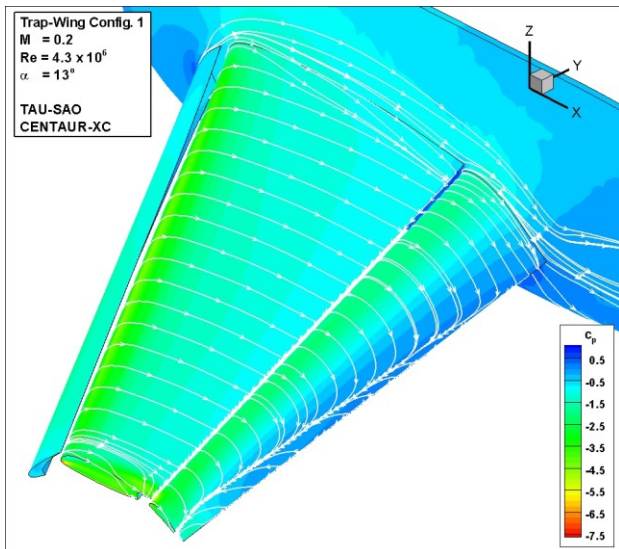
and 0.98

- TAU-SAO, grid-m; polar data



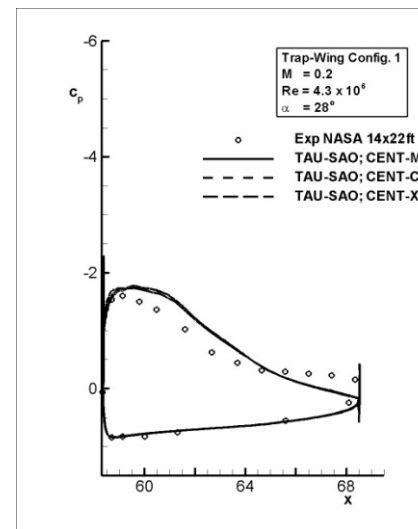
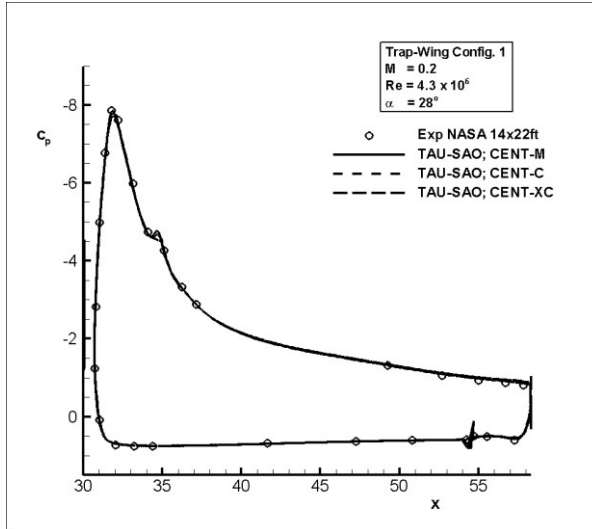
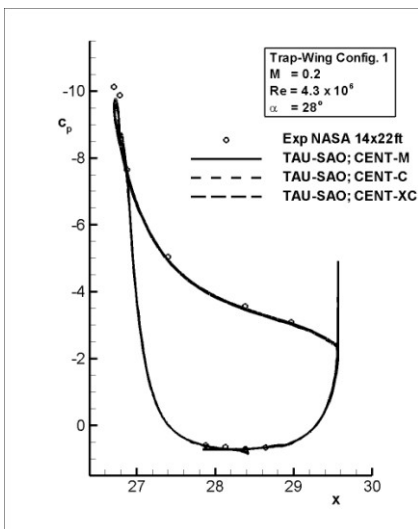
- TAU-SAO, grid-m; $\alpha = 13, 28^\circ$

isobars and surface streamlines

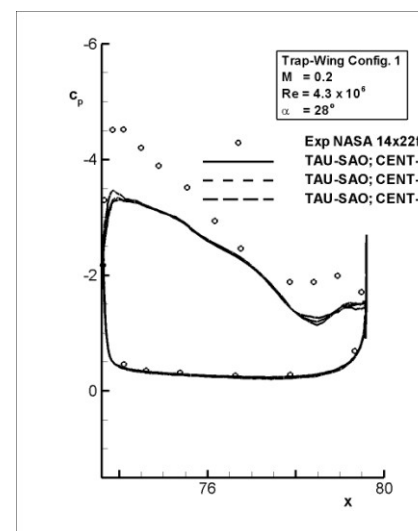
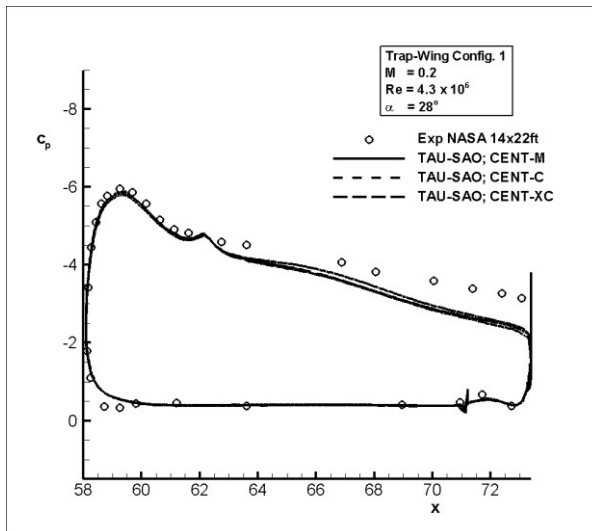
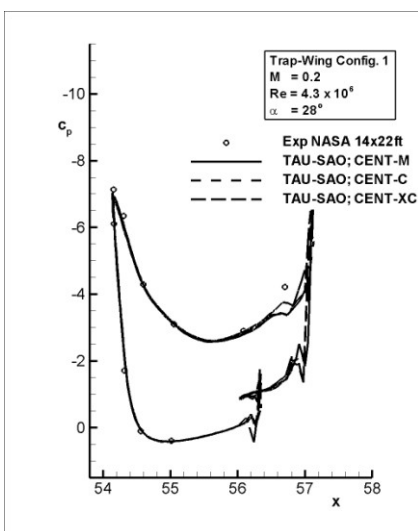


- TAU-SAO, grid-family; $\alpha = 28^\circ$:

pressure distribution at

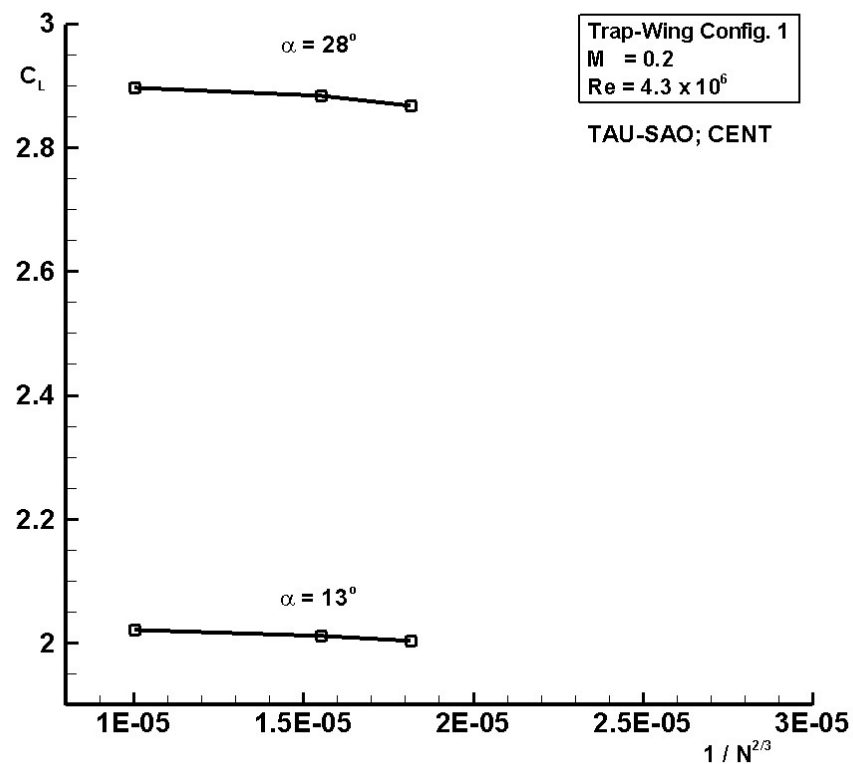
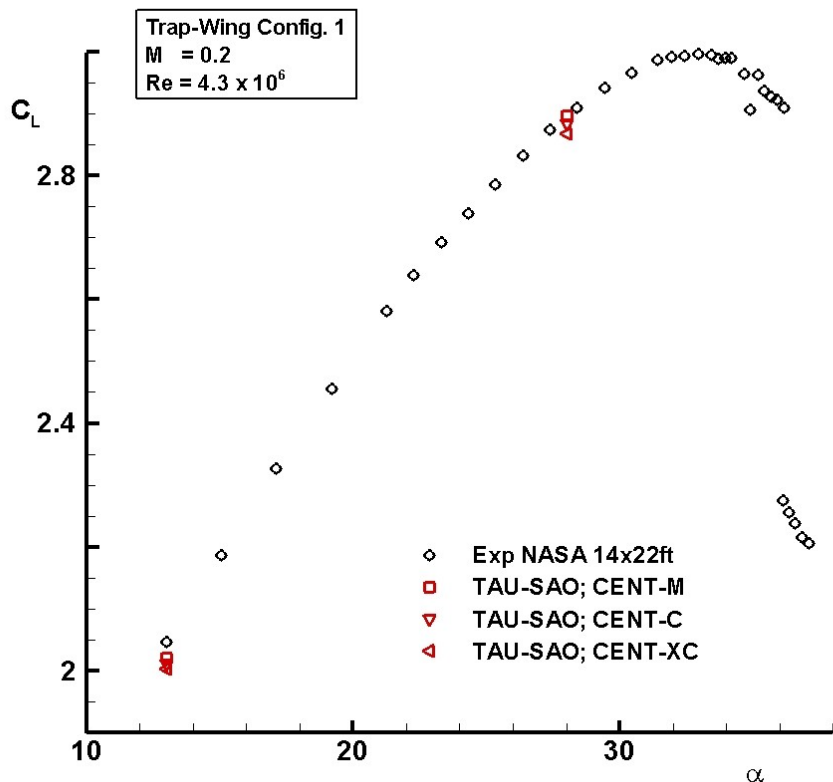


$\eta = 0.50$



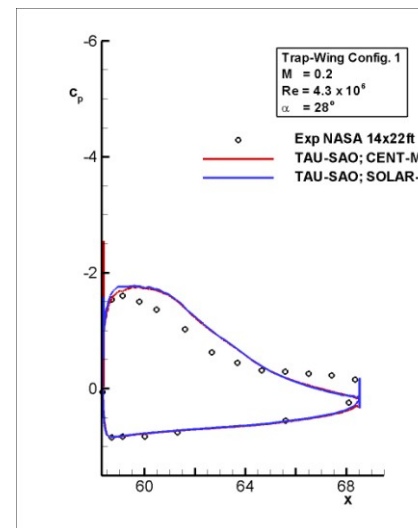
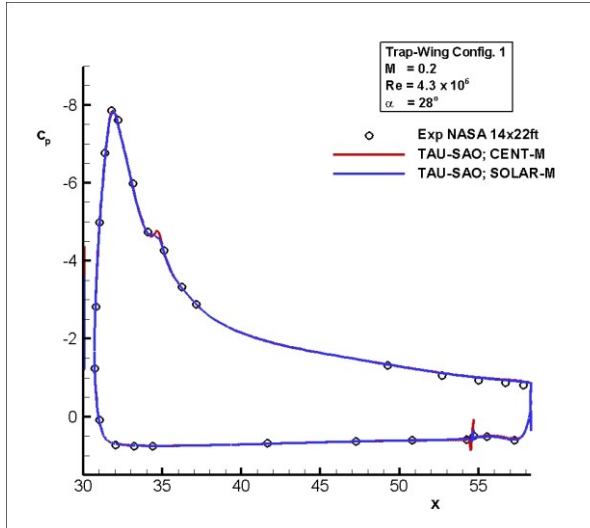
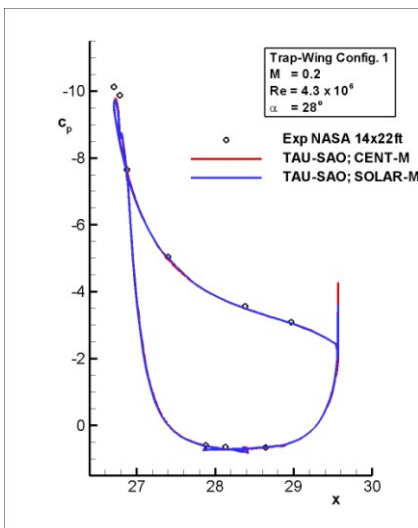
and 0.98

- TAU-SAO, grid-family; $\alpha = 13, 28^\circ$: lift force dependency

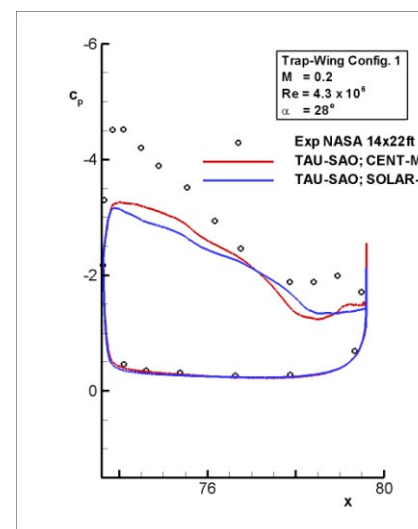
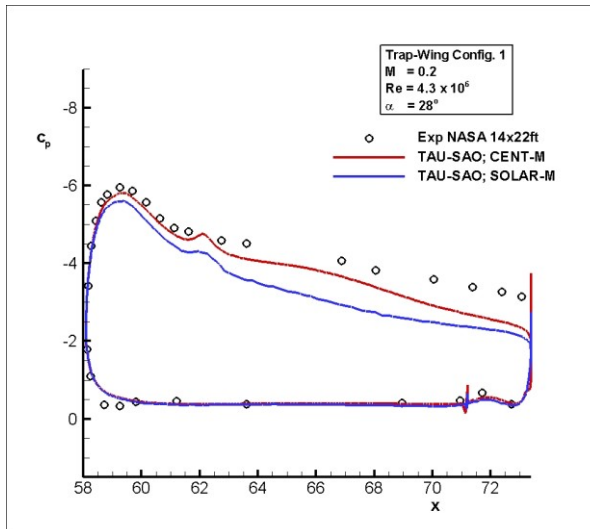
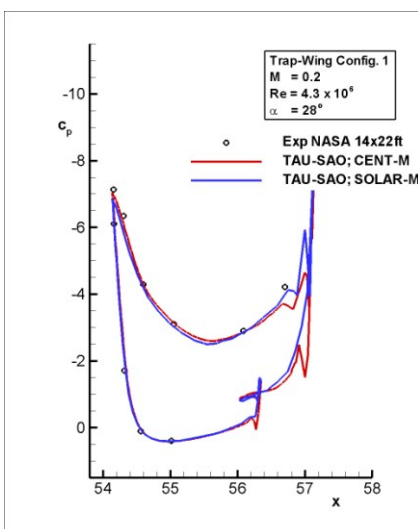


- TAU-SAO, grid-n; $\alpha = 28^\circ$: CENT/TAU vs. SOLAR/TAU

pressure distribution at

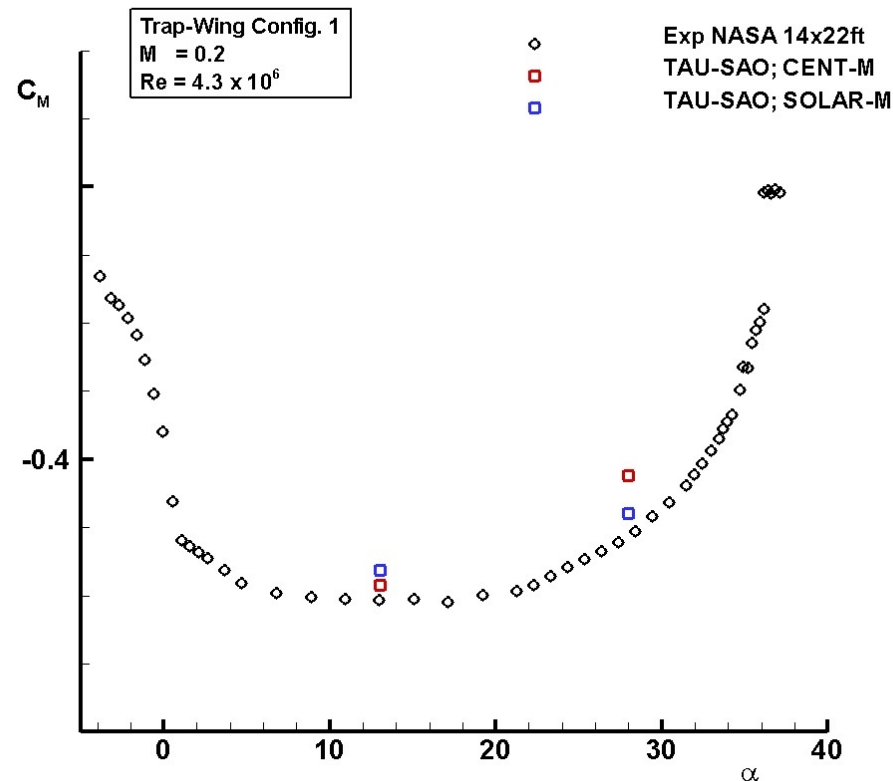
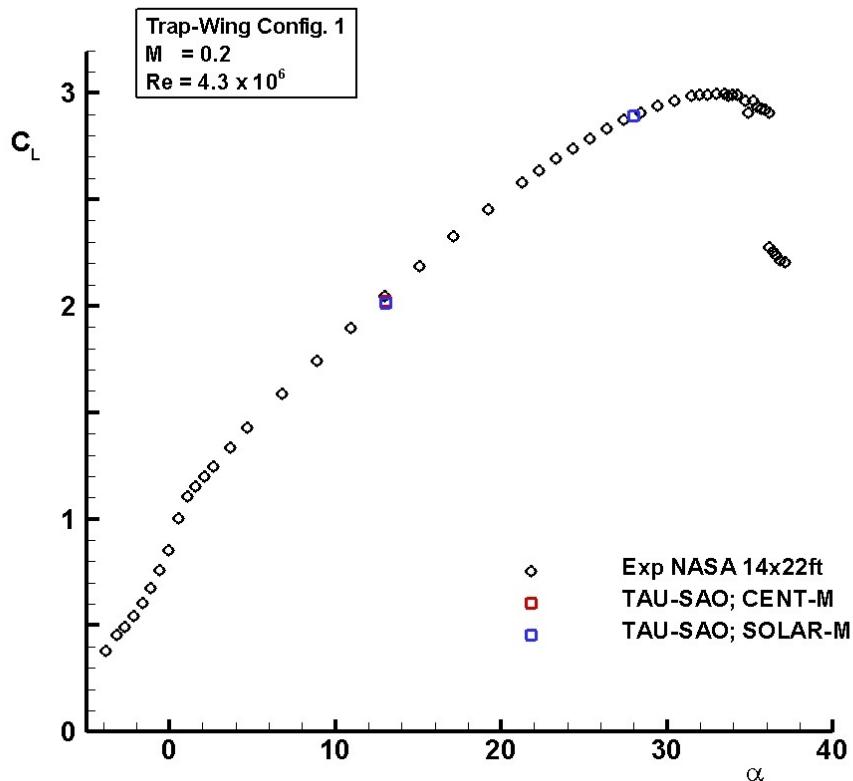


$\eta = 0.50$



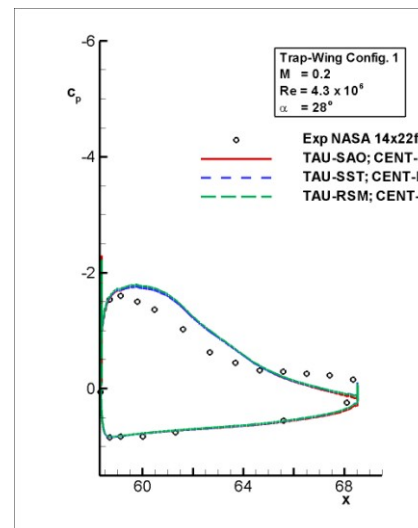
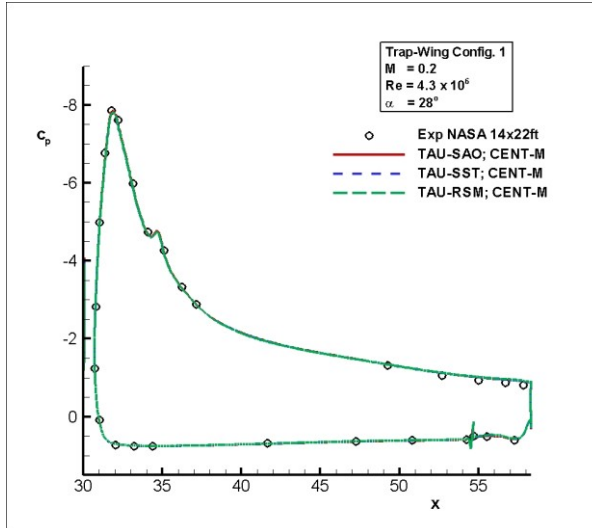
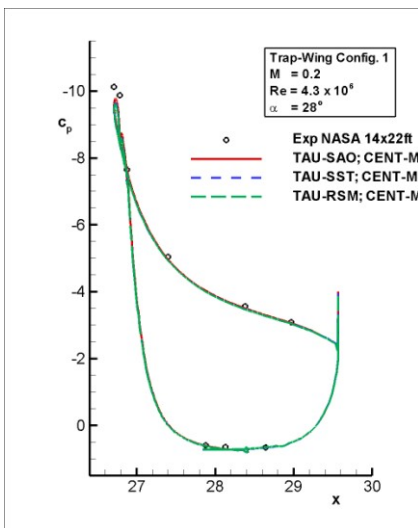
and 0.98

- TAU-SAO, grid-m; $\alpha = 13, 28^\circ$; CENT/TAU vs. SOLAR/TAU

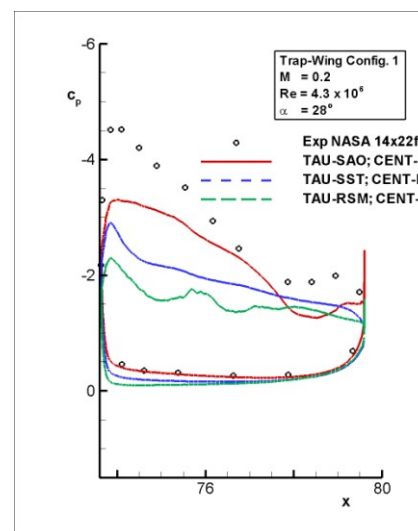
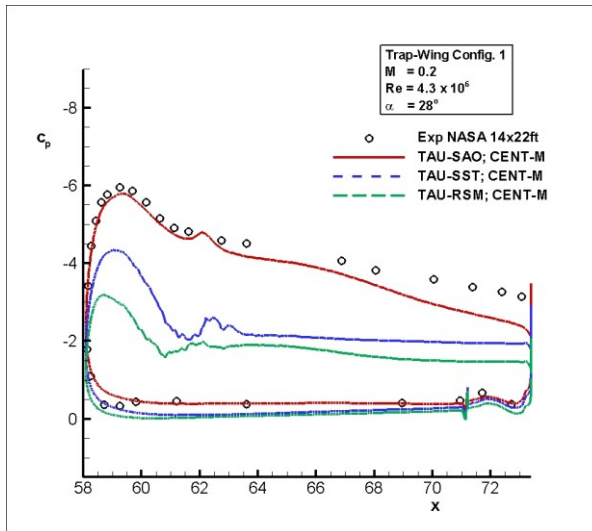
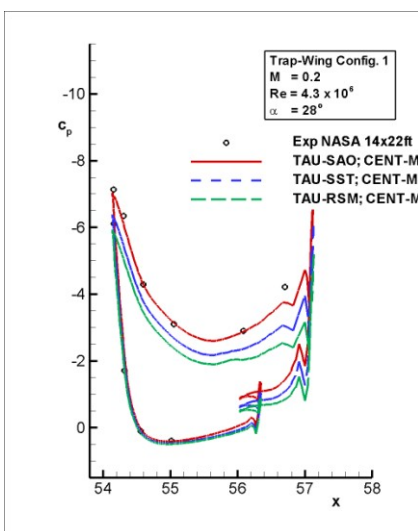


- TAU-SAO, grid-n; $\alpha = 28^\circ$: turb.-model-var.

pressure distribution at

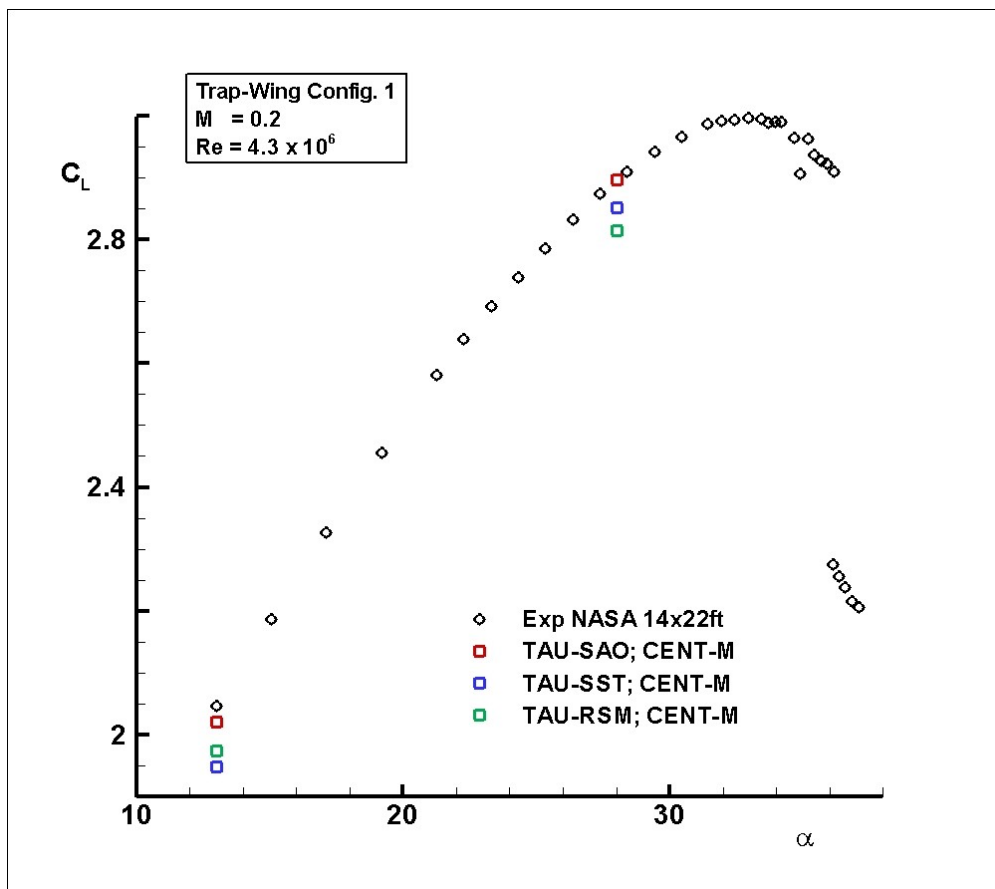


$\eta = 0.50$



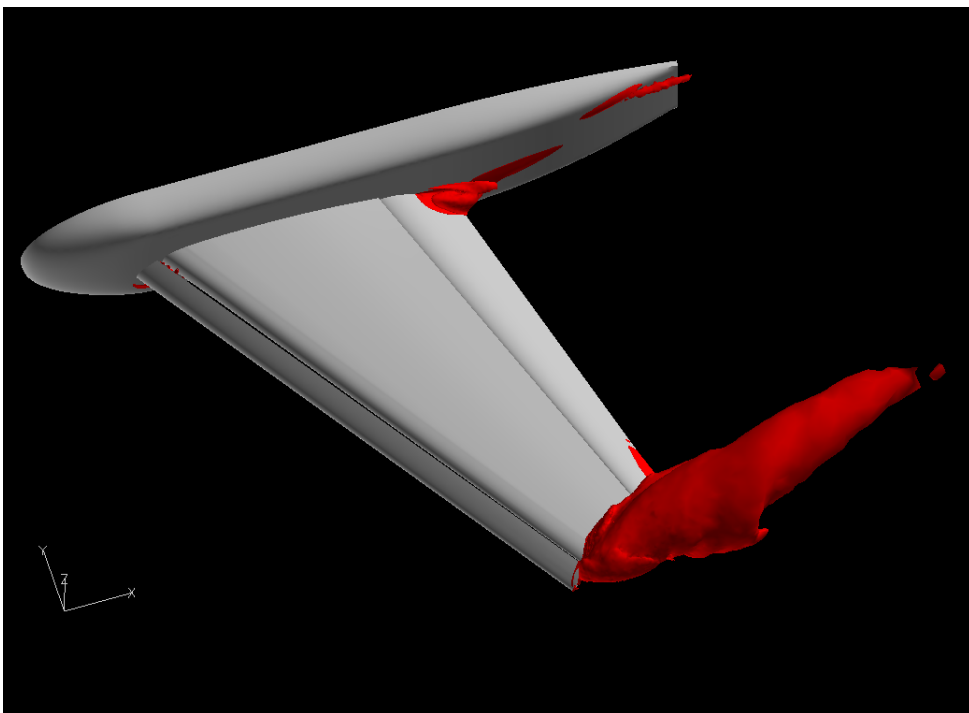
and 0.98

- TAU-SAO, grid-family; $\alpha = 13, 28^\circ$: turb.-model var.



- TAU, grid-m; $\alpha = 13^\circ$: Velocity difference field plots

TAU (SAO-SST)



TAU (SAO – RSM)

